

# Physico-Chemical Characterization, Opto Electronic Investigation and Vibrational Analysis on Coordinate Covalent Complex; Bis (Thiourea) Nickel Bromide (BTNB) Using Experimental and Computational Tools

Anand S<sup>1\*</sup>, Sundararajan RS<sup>2</sup>, Ramachandraraja C<sup>2</sup>, Ramalingam S<sup>1</sup> and Durga R<sup>1</sup>

<sup>1</sup>Department of Physics, AVC College, Mayiladuthurai, Tamil Nadu, India

<sup>2</sup>Department of Physics, Government Arts College, Kumbakonam, Tamil Nadu, India

## Abstract

In this work, a thorough spectroscopic investigation is made on the molecule; Bis (thiourea) Nickel Bromide (BTNB) by recording FT-IR, FT-Raman and UV Visible spectra. The computational calculations were carried out by HF and DFT methods with 6-31++G(d, p) and 6-311++G(d, p) basis sets and the optimized geometrical parameters, vibrational fundamentals, natural bond orbitals, Frontier molecular orbital energies and NMR chemical shift have been calculated and presented in the table. The cause of change of physical and chemical properties by coordination covalent bond between metal and organic atoms has been discussed in detail. Hence, the Non Linear Optical properties of the present molecule have been studied by calculating average Polarizability and diagonal hyperpolarizability. The enhancements of physical and chemical properties of the coordination complex due to the Vander Waals bond have been interpreted. The thermodynamical parameters were calculated and these values are obtained from NIST thermodynamical program. The variation of specific heat capacity, entropy and enthalpy with respect to different temperature are displayed in the graph and are discussed. A new semiorganic nonlinear optical crystal of Bis (thiourea) Nickel Bromide (BTNB) was grown successfully by slow evaporation technique using water as solvent. The lattice parameters of the grown crystal have been determined by X-ray diffraction studies. Vibrational spectrum is recorded to determine symmetries of molecular vibrations. The recording of Optical absorbance spectrum revealed that this crystal has good transparency in the visible region. The nonlinear nature of the present crystal has been confirmed by the SHG test. The BTNB crystal was analyzed by a differential thermal analysis and thermo gravimetric analysis (DTA-TGA) to obtain its thermal stability. Vickers micro-hardness test has done on the crystal and this shows that the crystal has greater physical strength.

**Keywords:** SHG; Micro hardness test; Vibrational investigation; NBO; BTNB

## Introduction

Nonlinear optical (NLO) frequency conversion materials have a significant impact on laser technology, optical communication and optical storage technology. The search for new frequency conversion materials over the past decade has led to the discovery of many semi organic NLO materials with high nonlinear susceptibilities. Among the semi organic NLO materials metal complexes of the thiourea having lower cut off wavelengths, applicable for frequency conversion are of very interest because both organic and inorganic components in it contribute specifically to the process of SHG [1-7]. In the present work, metal replacement is studied by taking a reported NLO crystal Bis (thiourea) Cadmium Bromide [8]. Here the metal cadmium is replaced by nickel which is more active electro chemically.

The preparation of crystals by combining the high non-linear optical activity of the organic molecules with the excellent physical properties of the inorganic molecule (metal compound) has been found to be overpoweringly successful in the recent past [9]. The thiourea molecule is an interesting inorganic matrix modifier due to its large dipole moment [10] and its ability to form an extensive network of hydrogen bonds [11]. The metal complexes of thiourea which have low UV cut off wavelengths, applicable for high power frequency conversion have received much attention. Ligands like thiourea form stable complexes through coordinated bonds by S and N donors which are adequate to combine with metal [12]. Now a day, many industries need such high efficiency crystals for many electric and electronic applications. Thiourea, which is otherwise centro-symmetric, yields excellent noncentro-symmetric materials and typifies this approach. Metal-organic compounds as NLO materials have attracted much more

attention for their high NLO coefficients, stable physical-chemical properties and better mechanical intension. Now a day, the production of NLO crystal materials using organic compounds with the addition of metal oxides has much attention due to its tremendous electronic and optical applications. Generally, the crystals made up of organic amine derivatives have rich NLO properties. The high symmetry organic amines derivatives; Thiourea has high NLO coefficients with stable physical and chemical properties. Generally, the metal oxide materials are able to have rich semiconducting properties and optical activities. When such metal oxides are coupled with thiourea, the physiochemical, electrical and optical properties are enriched. Due to the symmetrical presence of S and N donors in thiourea, the metal oxides are connected through coordinated covalent bonds strongly. It is a new attempt to fabricate metal organic compound; Bis (thiourea) Nickel Bromide (BTNB). After careful screening the literature, it is found that no quantum chemical computational work has been made on Bis (thiourea) Nickel Bromide (BTNB) so far. In this work, the

**\*Corresponding author:** Anand S, Department of Physics, AVC College, Mayiladuthurai, Tamil Nadu, India, Tel: 9443650530; E-mail: [anandphy09@gmail.com](mailto:anandphy09@gmail.com)

**Received** December 24, 2015; **Accepted** January 26, 2016; **Published** February 10, 2016

**Citation:** Anand S, Sundararajan RS, Ramachandraraja C, Ramalingam S, Durga R (2016) Physico-Chemical Characterization, Opto Electronic Investigation and Vibrational Analysis on Coordinate Covalent Complex; Bis (Thiourea) Nickel Bromide (BTNB) Using Experimental and Computational Tools. J Theor Comput Sci 3: 141. doi:10.4172/2376-130X.1000141

**Copyright:** © 2016 Anand S, et al. This is an open-access article distributed under the terms of the Creative Commons Attribution License, which permits unrestricted use, distribution, and reproduction in any medium, provided the original author and source are credited.

structural properties, vibrational study, frontier molecular analysis, NMR, UV-Visible spectral investigations have been carried out. The electrical, optical and chemical parameters have been calculated by using HF and DFT methods with 6-31++G(d, p) and 6-311++G(d, p) basis sets. The optical activity and NLO property analysis have been performed using appropriate quantum computational tools. Other industrial uses of thiourea include production of flame retardant resins and vulcanization accelerators. Thiourea is used as an auxiliary agent in light-sensitive photocopy paper and almost all other types of copy paper.

## Experimental and Computational Methods

### Instrumentation and synthesis

The compound BTNB is purchased from E-Merck, which is of spectroscopic grade and hence used for recording the spectra as such without any further purification. The FT-IR spectrum of the present compound is recorded in Bruker IFS 66V spectrometer in the range of 4000–100  $\text{cm}^{-1}$ . The spectral resolution is  $\pm 2 \text{ cm}^{-1}$ . The FT-Raman spectrum of AMS is also recorded in the same instrument with FRA 106 Raman module equipped with Nd:YAG laser source operating at 1.064  $\mu\text{m}$  line widths with 200 mW power. The spectra are recorded in the range of 4000–100  $\text{cm}^{-1}$  with scanning speed of 30  $\text{cm}^{-1} \text{ min}^{-1}$  of spectral width 2  $\text{cm}^{-1}$ . The frequencies of all sharp bands are accurate to  $\pm 1 \text{ cm}^{-1}$ . The Thermo Gravimetric Analysis and Differential Thermal Analysis (TGA and DTA) curves for BTNB were obtained using Simultaneous Thermo gravimetric Analyser (STA) 409C (NETZSCH) at a heating rate of 10°C/min in nitrogen. The absorption spectrum of BTNB was recorded using Varion Cary 5E UV-Vis-NIR spectrophotometer in the range 200-700 nm with high resolution. Single crystal XRD analysis was carried out using an Enraf Nonius CAD-4. X-ray diffractometer with  $M_oK_{\alpha}$  ( $\lambda=0.770 \text{ \AA}$ ) radiation to identify the structure and presence of functional groups in BTNB qualitatively, estimate lattice parameter values. The sample was in a pellet form in KBr phase. The nonlinear property of BTNB crystals was confirmed from second harmonic generation test by using Nd:YAG laser beam. The physical strength of the crystal was measured by Vicker's microhardness test.

The High purity salts (99.9%) purchased from E-Merck was used for the crystal growth experiments. Single crystals of Bis (thiourea) Nickel Bromide (BTNB) were grown at room temperature by slow evaporation of an aqueous solution containing thiourea and nickel bromide in stoichiometric ratio 2:1 as per the reaction. Colourless crystals were harvested in about 110 days and are shown in Figure 1.

### Computational procedure

Generally, quantum computational investigation tool with high degree of accuracy for vibrational spectral analysis is a comfortable instrument for doing physical and chemical parameter calculations to know the vibrational behaviour of a molecule. In this research work, the most fascinate level of theories; HF and DFT (B3LYP and B3PW91) were carried out using the basis sets 6-31++G(d, p) and 6-311++G(d, p). All these calculations were performed using GAUSSIAN 09W [13] program. In DFT methods; Becke's three parameter hybrids function combined with the Lee-Yang-Parr correlation function (B3LYP) [14,15], Becke's three parameter exact exchange-function (B3) [16] combined with gradient-corrected correlational functional of Lee, Yang and Parr (LYP) [17,18] and Perdew and Wang (PW91) [18,19] predict the best results for molecular geometry and vibrational frequencies for moderately larger molecules. The calculated frequencies are scaled down to yield results in coherent with the observed frequencies. The scaling factors are 0.84, 0.85, 0.87, 0.88 and 0.94 for HF/6-31++G/6-311++G(d,p) method. For DFT (B3LYP)/6-311++G(d, p) basis set, the

scaling factors are 0.90, 0.91, 0.93, 0.95 and 0.96. For DFT (B3PW91)/6-31++G/6-311++G(d,p) basis set, the scaling factors are 0.89, 0.90, 0.96, 0.97 and 0.98. The observed (FT-IR and FT-Raman) and calculated vibrational frequencies and vibrational assignments are submitted in Table 2. Experimental and simulated spectra of IR and Raman are presented in the Figures 2 and 3 respectively.

The  $^1\text{H}$  and  $^{13}\text{C}$  NMR isotropic chemical shift are calculated with the GIAO method [20] using the optimized parameters obtained from B3LYP/6-311++G(d, p) method.  $^{13}\text{C}$  isotropic magnetic shielding (TMS) of any X carbon atoms is made according to value  $^{13}\text{C}$  TMS,

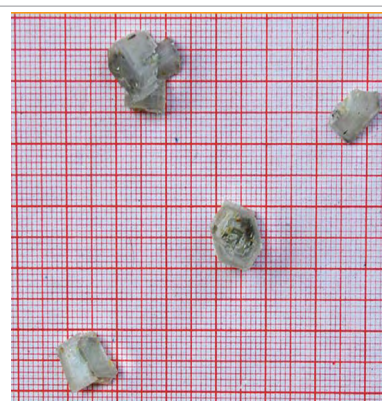


Figure 1: BTNB Crystals photograph.

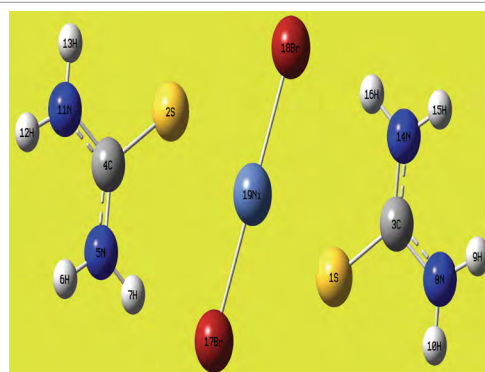


Figure 2: Molecular structure of Bis(thiourea) Nickel bromide.

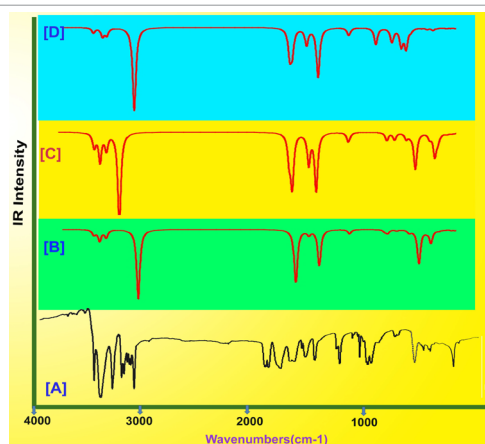


Figure 3: Experimental [A] and calculated [B, C and D] FT-IR spectra of Bis(thiourea) Nickel bromide (BTNB).

$CS_x = TMS_{TMS}$ . The  $^1H$  and  $^{13}C$  isotropic chemical shifts of TMS at B3LYP methods with 6-311++G(d,p) level using the IEFPCM method in DMSO, chloroform and  $CCl_4$ . The absolute chemical shift is found between isotropic peaks and the peaks of TMS [21].

The electronic and optical properties; HOMO-LUMO energies from IR and UV- Visible region, absorption wavelengths and oscillator strengths are calculated using B3LYP method of the time-dependent DFT (TD-DFT) [22-24], basing on the optimized structure in gas phase and solvent [DMSO, chloroform and  $CCl_4$ ] mixed phase. Thermodynamic properties have been calculated from 100-1000°C in gas phase using B3LYP/6-311++G (d, p) method. Moreover, the dipole moment, nonlinear optical (NLO) properties, linear polarizabilities and first order hyperpolarizabilities, chemical hardness, chemical softness and Electrophilicity index have also been studied.

## Results and Discussion

### Molecular geometry

The BTNB crystals belong to orthorhombic crystal class and point group of symmetry  $C_{2v}$ . The Ni ion is at the tetrahedral coordination site with two  $Br_2$  and two  $NH_2$  atoms at its top end. This gives rise to a three dimensional bonding network. All thiourea molecules are planar and are equidistant from the central Nickel atom. This structure gives a polymeric character to BTNB molecule with asymmetric units contributing additively to the effective nonlinearity. The molecular structure is optimized by Berny's optimization algorithm using Gauss view program and is shown in Figure 4. The comparative optimized structural parameters such as bond length, bond angle and dihedral angle are presented in Table 1. The present compound contains Nickel metal atom, bromide atoms and four amino groups.

The structure is optimized with different level of theory and the zero point vibrational energy of the compound in HF / B3LYP / B3PW91 and with 6-31++G (d, p) and 6-311++G (d, p) is 86.70, 84.90, 80.62, 80.10 and 79.51 Kcal/Mol respectively. The calculated energy of HF is greater than DFT method since the assumed ground state energy in HF is greater than the true energy. Since the existence of coordinate covalent bond between organic element and metal, molecular structure belongs to multiple planes with respect to Nickel bromide. The thiourea on both sides are somewhat tilted due to attraction between negatively charged Br and positively charged H. Since the present compound is

made up of metal atom and organic molecules, the entire atoms are connected by covalent and co-ordination covalent bonds. The Nickel metal atom is connected with couple of thiourea by Vander walls bonds. Normally, the metal ions make dative bond with organic atoms to form organo-metallic compound due to which the considerable amount of energy is released and make a crystal very strong.

The experimental bond length of C-S and C-N are 1.720 and 1.340 Å whereas the calculated bond lengths are 1.778 and 1.355 Å respectively. Though, both the amino groups are coupled with carbon symmetrically, the bond distance of C-N is differed by 0.0234 Å between them due to the attraction of H by Br. Normally, the double bond is to be between C and S atoms, but one bond alone is there due to 2 lone pair of electrons are transferred from ligand to metal (S to Ni). The calculated bond length of Ni - S is 2.352 Å called coordination covalent bond which is very high bond length when compared with others. The internuclear distance of N5 - H6 = N14 - H15 is 0.0139 Å which is greater than that of N5 - H7 = N14 - H16 Å due to the existence of Br and H attraction. From the optimized parameters, it is inferred that, the organo-metallic compound is very strong due to the complex bonds. The electrostatic force of attraction depending on the charges of the molecule has restricted the bond length which existed between metal and organic atoms. Such a force of attraction between metal and organic atom also affect the surrounding atoms of opposite signs. The highly electronegative bromine atoms are attracted much by the highly positive Nickel atoms.

### X-Ray diffraction studies

The single crystals of BTNB have been subjected to X-ray diffraction studies using an ENRAF NONIUS CAD4 X-ray diffractometer to determine the cell parameters. The studies revealed that the crystal belongs to orthorhombic system. In order to understand the role of metal ions in the grown crystals, a comparison is made between free ligand thiourea and Bis (thiourea) Nickel Bromide and is given in Table 3. The data reveals the fact that BTNB crystals possess smaller volume when compared with bithiourea. This may be due to smaller atomic radius of nickel bromide when compared with bithiourea.

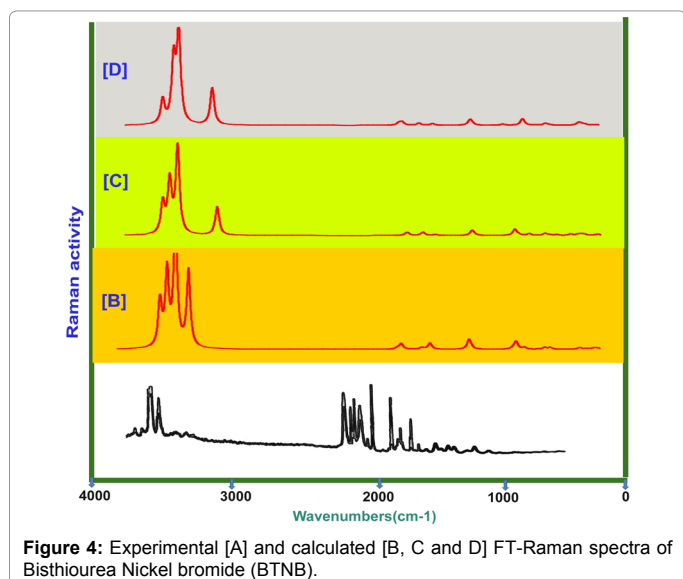
### Vibrational assignments

In order to obtain the spectroscopic signature of the BTNB crystal, the computational calculations are carried out for frequency analysis. The molecule is identified with  $C_{2v}$  point group symmetry, consists of 19 atoms, so it has 51 normal vibrational modes. On the basis of  $C_{2v}$  symmetry, the 51 fundamental vibrations of the molecule can be distributed as

$$\Gamma \text{ Vib} = 19A_1 + 7A_2 + 11B_1 + 14B_2$$

$A_1$  and  $B_2$  irreducible representations correspond to stretching, ring deformation and in-plane bending vibrations while  $A_2$  and  $B_1$  correspond to ring, torsion and out-of-plane bending vibrations. The harmonic vibrational frequencies (unscaled and scaled) calculated at B3LYP and B3PW91 levels using the triple split valence basis set along with the diffuse and polarization functions; 6-31++G(d,p) and 6-311++G(d,p) and observed FT-IR and FT-Raman frequencies for various modes of vibrations have been presented in Tables 2 and 4 respectively. Comparison of calculated frequencies with the experimental values reveal the over estimation of the calculated vibrational modes due to the neglect of a harmonicity and change of state of real system.

**Amino group vibrations:** The molecule thiourea consists of couple of  $NH_2$  groups on both sides; there are eight N-H stretching vibrations



Geometrical Parameters	Methods				
	HF		B3PW91		B3LYP
	6-31++G (d-p)	6-311++G (d-p)	6-31++G (d-p)	6-311++G (d-p)	6-311++G (d-p)
<b>Bond length(Å)</b>					
(S1-C3)	1.7134	1.7146	1.7047	1.7063	1.778
(S1-Ni19)	2.5206	2.4857	2.2279	2.2486	2.3525
(S2-C4)	1.7134	1.7146	1.7192	1.7063	1.778
(S2-Ni19)	2.5206	2.4859	2.2521	2.2487	2.3524
(C3-N8)	1.3336	1.3335	1.3513	1.3521	1.3558
(C3-N14)	1.3177	1.315	1.3316	1.3268	1.3324
(C4-N5)	1.3177	1.315	1.326	1.3268	1.3324
(C4-N11)	1.3336	1.3335	1.3535	1.3521	1.3558
(N5-H6)	0.9947	0.9941	1.009	1.0072	1.0082
(N5-H7)	1.0014	1.0019	1.0334	1.0269	1.0221
(N8-H9)	0.9939	0.9934	1.0081	1.0075	1.0066
(N8-H10)	0.9932	0.9926	1.0074	1.0068	1.0051
(N11-H12)	0.9939	0.9934	1.0085	1.0075	1.0066
(N11-H13)	0.9932	0.9926	1.008	1.0068	1.0051
(N14-H15)	0.9947	0.9941	1.0079	1.0072	1.0082
(N14-H16)	1.0014	1.0019	1.0264	1.0269	1.0221
(Br17-Ni19)	2.3854	2.4351	2.2886	2.3438	2.3954
(Br18-Ni19)	2.3855	2.435	2.3046	2.3437	2.3954
<b>Bond angle(°)</b>					
(C3-S1-Ni19)	115.1831	117.5015	108.6219	115.6933	120.4865
(C4-S2-Ni19)	115.178	117.5084	121.4044	115.688	120.4846
(S1-C3-N8)	118.1165	117.3579	117.4085	116.4575	115.7425
(S1-C3-N14)	124.1006	124.754	124.5733	125.6001	125.6174
(N8-C3-N14)	117.7828	117.888	118.0145	117.9163	118.6381
(S2-C4-N5)	124.1009	124.7553	125.9546	125.599	125.6159
(S2-C4-N11)	118.1168	117.3584	115.9481	116.4595	115.7432
(N5-C4-N11)	117.7822	117.8863	118.089	117.9155	118.6388
(C4-N5-H6)	121.5291	121.4406	120.888	121.3556	122.524
(C4-N5-H7)	119.8174	119.8712	117.4465	118.1593	118.8815
(H6-N5-H7)	118.0455	118.4276	119.5277	120.0647	118.5514
(C3-N8-H9)	122.3462	122.1864	121.0284	120.4874	122.6564
(C3-N8-H10)	118.8558	118.835	117.5071	117.1188	119.1289
(H9-N8-H10)	118.7808	118.8106	117.8149	117.5872	118.2004
(C4-N11-H12)	122.3468	122.1827	120.4589	120.4856	122.6562
(C4-N11-H13)	118.8562	118.8323	116.9425	117.118	119.1293
(H12-N11-H13)	118.7816	118.8084	117.2405	117.5859	118.2001
(C3-N14-H15)	121.5305	121.4403	121.6115	121.3561	120.4846
(C3-N14-H16)	119.8182	119.8695	117.4945	118.1601	122.524
(H15-N14-H16)	118.0467	118.4264	120.1559	120.0641	118.882
(S1-Ni19-S2)	118.8248	142.8057	168.847	179.9937	118.5509
(S1-Ni19-Br17)	91.0995	87.0194	86.6128	84.8925	174.7149
(S1-Ni19-Br18)	105.4523	102.2402	92.5926	95.1095	81.6934
(S2-Ni19-Br17)	105.4587	102.2399	100.0479	95.1021	98.7543
(S2-Ni19-Br18)	91.1022	87.0255	82.7305	84.8959	98.7515
<b>Dihedral angles(°)</b>					
(Ni19-S1-C3-N8)	170.9494	168.7332	155.9976	161.0783	172.5991
(Ni19-S1-C3-N14)	-8.9451	-11.2467	-23.29	-17.0157	-6.875
(C3-S1- Ni19-S2)	-74.112	-75.9729	-0.3341	-102.1257	-74.9862
(C3-S1- Ni19-Br17)	177.5358	177.6138	-127.4452	-132.3125	-170.2066
(C3-S1- Ni19-Br18)	25.961	25.4491	64.5039	47.6923	19.4797
(Ni19-S2-C4-N5)	-8.939	-11.2744	-15.9644	17.0323	-6.8895
(Ni19-S2-C4-N11)	170.9586	168.7043	165.1017	-161.0637	172.585
(C4-S2- Ni19-S1)	-74.0963	-75.9863	-115.8085	-77.9027	-74.9181
(C4-S2- Ni19-Br17)	25.9774	25.4247	10.2444	-47.7163	19.5119
(C4-S2- Ni19-Br18)	177.5574	177.5916	178.4767	132.2789	-170.1745
(S1-C3-N8-H9)	178.1378	175.602	157.8652	157.5191	177.1446

(S1-C3-N8-H10)	-0.3327	0.3712	-0.1326	2.656	-1.4494
(N14-C3-N8-H9)	-1.961	-4.4167	-22.7993	-24.2346	-3.3424
(N14-C3-N8-H10)	179.5685	-179.6475	179.2029	-179.0977	178.0635
(S1-C3-N14-H15)	-177.1744	-178.4869	175.7644	174.3705	177.9032
(S1-C3-N14-H16)	-6.2639	-4.4795	-14.0677	-13.0624	-4.5214
(N8-C3-N14-H15)	2.9308	1.5333	-3.5192	-3.6985	-1.5571
(N8-C3-N14-H16)	173.8413	175.5406	166.6486	168.8687	176.0183
(S2-C4-N5-H6)	-177.1639	-178.505	170.7307	-174.3695	177.8959
(S2-C4-N5-H7)	-6.2786	-4.4615	7.4289	13.0692	-4.5279
(N11-C4-N5-H6)	2.9381	1.5164	-10.3559	3.7015	-1.5648
(N11-C4-N5-H7)	173.8234	175.5599	-173.6577	-168.8598	176.0115
(S2-C4-N11-H12)	178.1865	175.5286	159.4851	-157.5019	177.1336
(S2-C4-N11-H13)	-0.3699	0.4181	6.0329	-2.6485	-1.4564
(N5-C4-N11-H12)	-1.9093	-4.4912	-19.5367	24.2501	-3.3532
(N5-C4-N11-H13)	179.5343	-179.6017	-172.9889	179.1035	178.0569

Table 1: Optimized geometrical parameters for Bis(thiourea) Nickel Bromide (BTNB) computed at HF, DFT (B3LYP & B3PW91) with 6-31++G(d, p) & 6-311++G(d, p) basis sets.

S. No	Symmetry Species $C_{2v}$	Observed Frequency( $cm^{-1}$ )		Methods					Vibrational Assignments
				HF		B3PW91		B3LYP	
		FTIR	FT-Raman	6-31++G (d, p)	6-311++G (d, p)	6-31++G (d, p)	6-311++G (d, p)	6-311++G (d, p)	
1	$A_1$	3340 s	3340 s	3336	3356	3338	3349	3343	(N-H) $\nu$
2	$A_1$	3335 vs	3335 s	3336	3356	3330	3349	3343	(N-H) $\nu$
3	$A_1$	3315 vs	3315 m	3321	3303	3318	3297	3296	(N-H) $\nu$
4	$A_1$	3305 s	-	3321	3303	3300	3397	3296	(N-H) $\nu$
5	$A_1$	3285 s	-	3284	3281	3254	3273	3256	(N-H) $\nu$
6	$A_1$	3270 s	-	3284	3281	3249	3273	3256	(N-H) $\nu$
7	$A_1$	3260 s	3260 w	3258	3234	3242	3267	3231	(N-H) $\nu$
8	$A_1$	3235 vs	3235 w	3232	3231	3214	3228	3227	(N-H) $\nu$
9	$A_1$	1620 s	1620 m	1613	1604	1607	1607	1622	(N-H) $\delta$
10	$A_1$	1600 m	1600 m	1594	1604	1590	1604	1619	(N-H) $\delta$
11	$A_1$	1585 s	-	1582	1576	1588	1597	1579	(N-H) $\delta$
12	$B_2$	1560 s	-	1563	1557	1570	1563	1562	(N-H) $\delta$
13	$B_2$	1540 w	1540 vs	1534	1534	1538	1516	1536	(N-H) $\delta$
14	$A_1$	1480 m	-	1466	1478	1472	1470	1472	(N-H) $\delta$
15	$A_1$	1470 s	-	1463	1469	1467	1468	1442	(N-H) $\delta$
16	$A_1$	1455 w	1455 s	1444	1452	1445	1464	1430	(N-H) $\delta$
17	$A_1$	1410 s	-	1400	1405	1406	1427	1404	(N-H) $\delta$
18	$A_1$	1370 s	-	1363	1368	1366	1361	1359	(C-N) $\nu$
19	$B_2$	1305 s	1305 s	1300	1298	1303	1294	1311	(C-N) $\nu$
20	$B_2$	1250 s	1250 m	1242	1239	1237	1240	1246	(C-N) $\nu$
21	$B_2$	1235 m	1235 m	1232	1220	1229	1230	1237	(C-S) $\nu$
22	$B_2$	1200 w	-	1192	1220	1188	1198	1193	(C-S) $\nu$
23	$B_2$	1190 s	-	1184	1204	1186	1187	1191	(C-N) $\nu$
24	$B_2$	980 m	980 w	976	978	974	988	993	(N-H) $\gamma$
25	$B_1$	850 m	-	845	845	826	859	851	(N-H) $\gamma$
26	$B_1$	730 s	730 s	723	727	740	735	728	(Ni-Br) $\nu$
27	$A_2$	695 s	700 s	690	690	663	683	676	(Ni-Br) $\nu$
28	$A_2$	640 s	-	638	630	646	631	619	(N-H) $\gamma$
29	$A_2$	605 m	-	608	606	626	625	602	(N-H) $\gamma$
30	$A_2$	550 w	-	546	554	565	573	549	(N-H) $\gamma$
31	$B_2$	515 w	-	514	510	548	546	502	(N-H) $\gamma$
32	$B_2$	500 m	-	502	506	531	530	498	(Ni-Br) $\nu$
33	$A_1$	470 m	470 w	456	449	502	462	441	(Ni-Br) $\nu$
34	$A_1$	430 w	-	427	446	450	457	429	(Ni-S) $\nu$
35	$A_1$	405 m	-	404	408	410	367	392	(Ni-S) $\nu$
36	$B_2$	390 m	390 w	389	379	362	375	390	(C-N) $\delta$
37	$B_2$	380 w	380 w	377	377	373	368	358	(C-N) $\delta$
38	$A_2$	350 w	-	333	328	344	339	348	(C-S) $\delta$
39	$A_2$	315 m	315 w	307	296	303	307	310	(C-S) $\delta$

40	A <sub>2</sub>	280 m	280 w	270	281	282	280	286	(Ni-Br) δ
41	B <sub>2</sub>	260 w	-	248	256	266	256	262	(Ni-Br) δ
42	B <sub>2</sub>	210 w	210 vw	207	211	205	176	154	(Ni-S) δ
43	B <sub>1</sub>	200 w	200 vw	122	130	184	160	143	(Ni-S) δ
44	B <sub>1</sub>	180 w	-	111	110	142	138	131	(C-N) γ
45	B <sub>1</sub>	160 w	-	92	97	137	137	121	(C-N) γ
46	B <sub>1</sub>	150 w	-	87	89	114	116	100	(C-S) γ
47	B <sub>1</sub>	135 w	-	73	53	62	56	62	(C-S) γ
48	B <sub>1</sub>	125 w	125 vw	59	47	55	53	61	(Ni-Br) γ
49	B <sub>1</sub>	100 w	100 vw	54	35	35	29	32	(Ni-Br) γ
50	B <sub>1</sub>	90 w	-	44	35	25	22	14	(Ni-S) γ
51	B <sub>1</sub>	80 w	-	21	15	8	10	9	(Ni-S) γ

s – Strong; m- Medium; w – weak; as- Asymmetric; s – symmetric; u – stretching; α – deformation, δ - In plane bending; γ-out plane bending; τ – Twisting;

**Table 2:** Observed and calculated vibrational frequencies of Bis(thiourea) Nickel Bromide (BTNB) with HF & DFT (B3LYP & B3PW91) method at 6-31++G(d, p) & 6-311++G(d, p) basis set.

S. No	Sample	a (Å)	b (Å)	c (Å)	A (°)	B (°)	Γ (°)	Volume (Å <sup>3</sup> )
1	Thiourea	7.655	8.537	5.520	90	90	90	360.732
2	BTNB	6.1310	8.0907	9.1131	90	90	90	352.838

**Table 3:** A comparison of Lattice Parameters of Thiourea and Bis(thiourea) Nickel Bromide (BTNB).

possible. Normally, aliphatic primary amines are characterized by strong absorption in the region of 3450 – 3100 cm<sup>-1</sup> due to the asymmetric and symmetric NH<sub>2</sub><sup>+</sup> stretching. Specifically, the symmetric N–H stretching vibrations occur in the region 3100 – 3300 cm<sup>-1</sup> [25]. The asymmetric N–H<sub>2</sub> stretching vibration appeared from 3300 – 3500 cm<sup>-1</sup> and the symmetric NH<sub>2</sub> stretching is observed in the range 3350 – 3420 cm<sup>-1</sup> [26]. Also the NH<sub>2</sub><sup>+</sup> asymmetric and symmetric deformation wave numbers are expected to fall in the regions 1660 – 1610 cm<sup>-1</sup> and 1550 – 1485 cm<sup>-1</sup>, respectively [27,28]. In the present case, the N–H stretching frequencies are observed at 3340, 3335, 3315, 3305, 3285, 3270, 3260 and 3235 cm<sup>-1</sup>. The first three bands and second five bands are assigned to asymmetric and symmetric vibrations respectively. In addition to that, last two vibrational bands are found to be moved down from the expected region. This is mainly due to the presence of sulphur with chain. The N–H in-plane bending vibrations (scissoring) are usually observed in the region 1610 – 1630 cm<sup>-1</sup>, rocking vibrations are assigned in the range 1100 – 1200 cm<sup>-1</sup> and the out-of-plane bending (wagging and twisting) vibrations are normally identified under 1150 – 900 cm<sup>-1</sup> [29-31]. The in-plane deformation vibrations for the present compound is observed at 1620, 1600, 1585, 1560, 1540, 1480, 1470, 1455 and 1410 cm<sup>-1</sup>. The first two bands are moved up to the higher region and it is cleared that, these vibrations is favoured. The out-of-plane bending vibrations are set up at 980, 850, 640, 605, 550 and 515 cm<sup>-1</sup>. Normally, whenever the metal atom coupled with the organic molecules, the normal vibrational modes of the same are suppressed much. The entire out-of-plane bending vibrations are found out of the expected region. This view clearly shows that the N–H out-of-plane vibrations hindering by other vibrations. From the N–H vibrations, it is observed that, the entire out-of-plane vibrational modes affected by other substitutions in the chain.

**C–N vibrations:** The C–N stretching frequency is rather a difficult task since there are problems in identifying these frequencies from other vibrations [32]. Silverstein [33] assigned C–N stretching vibrations in the region 1386 – 1266 cm<sup>-1</sup> for aromatic amines. In this work, the C–N Stretching is observed at 1370, 1305, 1250 and 1190 cm<sup>-1</sup> which is making disagreement with the literature [34] due to the loading of sulphur and metal atoms with the molecule. The C–NH<sub>2</sub> in-plane and out-of-plane bending vibrations are appeared at 390 and 380 and 180 and 160 cm<sup>-1</sup> respectively. These two vibrations are affected

much by other vibrations which make disagreement with literature values [35,36].

**C–S vibrations:** The thio-cyanate ion may act as an ambidentate ligand, i.e., bonding may occur either through the nitrogen or the sulphur atom. The bonding mode may easily be distinguished by examining the band due to the C–S stretching vibration which occurs at 730 – 690 cm<sup>-1</sup> [37-39] when the bonding occurs through the sulphur atom and at 860 – 780 cm<sup>-1</sup> when it is through the nitrogen atom. In the present case, the C–S stretching vibrations are identified with medium intensity at 1235 and weak intensity at 1200 cm<sup>-1</sup> in IR spectrum. The observed bands are in line with the expected range and literature [40]. Generally, The C–S in-plane bending vibrations are observed in the 440 – 410 cm<sup>-1</sup> [40]. In this metal organic compound, the in-plane bending vibrations are found at 350 and 315 cm<sup>-1</sup> and the out-of-plane bending vibrations at 150 and 135 cm<sup>-1</sup>. These vibrational bands are pulled down to the lower region of the expected range due to the Nickel ion.

**Ni–Br and Ni–S vibrations:** The present molecule is a metal-organic crystal compound which comprises nickel metal ion linked with couple of bromine atoms by forming coordinate covalent bond. Generally, in Nickel metal complex, the Ni–Br stretching is very significant. In this compound, the coordinate covalent bond stretching vibrations are identified at 730, 695, 500 and 470 cm<sup>-1</sup>. The Ni–Br in-plane and out-of-plane bending vibrational peaks have appeared at 280 and 260 cm<sup>-1</sup> and 125 and 100 cm<sup>-1</sup> respectively. From the Ni–Br vibrations, it is inferred that, these vibrations are elevated to higher region. This view clearly shows that, the metal-organic inter nuclear distance are made up of coordinate covalent bond and usually these vibrations will not be affected in order to emphasize its uniqueness character.

In the present molecule, the organic compound; bithiourea is directly connected through sulphur atom with metal chloride by forming coordinate covalent bond as S–Ni–S. Usually the Ni–S vibrations are pushed to the higher region by organic vibrations due to the large force constants and strong covalent bond. The Ni–S bond is made up of coordinate covalent bond which is a very weak bond, its vibrations fallback to the Ni–Br vibrations. In the present case, the Ni–S stretching vibrations are observed at 430 and 405 cm<sup>-1</sup>. The corresponding in-plane and out-of-plane bending vibrations

S. No	Observed frequency	Calculated frequency				
		HF		B3PW91		B3LYP
		6-31++G (d, p)	6-311++G (d, p)	6-31++G (d, p)	6-311++G (d, p)	6-311++G (d, p)
1	3340	3972	3949	3751	3722	3715
2	3335	3972	3949	3742	3722	3715
3	3315	3908	3886	3687	3664	3622
4	3305	3908	3886	3667	3664	3622
5	3285	3832	3816	3616	3597	3579
6	3270	3832	3816	3610	3597	3579
7	3260	3716	3675	3309	3267	3297
8	3235	3715	3672	3183	3261	3293
9	1620	1834	1823	1674	1657	1708
10	1600	1833	1823	1657	1654	1705
11	1585	1798	1791	1655	1647	1680
12	1560	1797	1790	1653	1646	1680
13	1540	1615	1610	1538	1516	1536
14	1480	1612	1607	1518	1516	1534
15	1470	1540	1531	1425	1412	1442
16	1455	1537	1529	1417	1408	1416
17	1410	1187	1181	1116	1098	1106
18	1370	1186	1180	1102	1098	1105
19	1305	1161	1159	1086	1079	1093
20	1250	1161	1158	1076	1079	1093
21	1235	790	763	793	737	825
22	1200	790	761	743	735	823
23	1190	764	753	719	707	662
24	980	763	753	696	706	662
25	850	693	676	636	614	655
26	730	689	674	617	613	650
27	695	566	548	510	488	564
28	640	565	548	497	486	563
29	605	507	505	482	481	515
30	550	506	504	471	478	514
31	515	459	464	457	455	466
32	500	457	460	443	442	462
33	470	456	449	419	385	441
34	430	455	446	375	381	429
35	405	321	292	342	306	357
36	390	267	237	302	268	355
37	380	264	236	267	263	299
38	350	196	205	246	261	240
39	315	181	185	217	205	194
40	280	180	176	202	200	191
41	260	138	160	190	183	175
42	210	138	132	171	176	154
43	200	122	130	154	160	143
44	180	111	110	142	138	131
45	160	92	97	137	137	121
46	150	87	89	114	116	100
47	135	73	53	62	56	62
48	125	59	47	55	53	61
49	100	54	35	35	29	32
50	90	44	35	25	22	14
51	80	21	15	10	10	9

**Table 4:** Calculated unscaled frequencies of Bis (thiourea) Nickel Bromide (BTNB) computed at HF, B3LYP & B3PW91 with 6-31++G(d, p) & 6-311++G(d, p) basis sets.

are found at 210 and 200  $\text{cm}^{-1}$  and 90 and 80  $\text{cm}^{-1}$  respectively. The entire vibrations of Ni-S are observed in the lower region of the IR spectrum which shows the weak attraction of the bond between the metal and organic compound. Though the bond is weak, the crystal and chemical properties of the present compound are good. So, the crystal compound possesses piezo electric effect that can be used for electric and electronic applications.

### NMR Assessment

NMR spectroscopy technique is throwing a new light on organic structure elucidation of much difficult complex molecules. The combined use of experimental and computational tools offers a powerful gadget to interpret and predict the structure of bulky molecules. The optimized structure of BTNB is used to calculate the NMR spectra at B3LYP method with 6-311++G (d, p) level using the GIAO method and the chemical shifts of the compound are reported in ppm relative to TMS for  $^1\text{H}$  and  $^{13}\text{C}$  NMR spectra which are presented in Table 5. The corresponding spectra are shown in Figure 5.

Normally, the range of  $^{13}\text{C}$  NMR chemical shifts for aromatic derivatives is greater than 100 ppm and the accuracy ensures that the reliable interpretation of spectroscopic parameters. In the present

work, the metallo organic compound has been taken for the study in which the molecule contains two carbons along with two amine group. The  $^{13}\text{C}$  NMR chemical shift of such two carbons is greater than 100 ppm, as in the expected regions.

In the case of BTNB, the chemical shift of C3 and C4 are 164.29 and 164.72 ppm respectively. Here, the chemical shift is same for C3 and C4 since both the carbons having similar groups. The chemical shift of both carbons is very high; it is also due to the migration of double bond from C-S to C-N. The chemical shift of Br (4033.39) is finite and apparently high due to the random breaking of proton shield by the fusing of coordinate covalent bond with organic molecules. The chemical shift of H6, H7, H9, H10, H12, H13, H15 and H16 are 25.27, 12.81, 24.63, 22.75, 24.68, 19.79, 25.20 and 12.71 ppm respectively. From the result of shift in Hydrogen atom, it is observed that, the chemical shift of H7, H13 and H16 are lower than the rest of other hydrogen atoms in the chain. This is purely due to the extended influence on hydrogen atom by nearby bromine atoms. From the entire chemical shift of the molecules, it can be inferred that, the chemical property of the metal is directly mingled with organic molecules and this is the main cause for the present metal complex molecule having new chemical property.

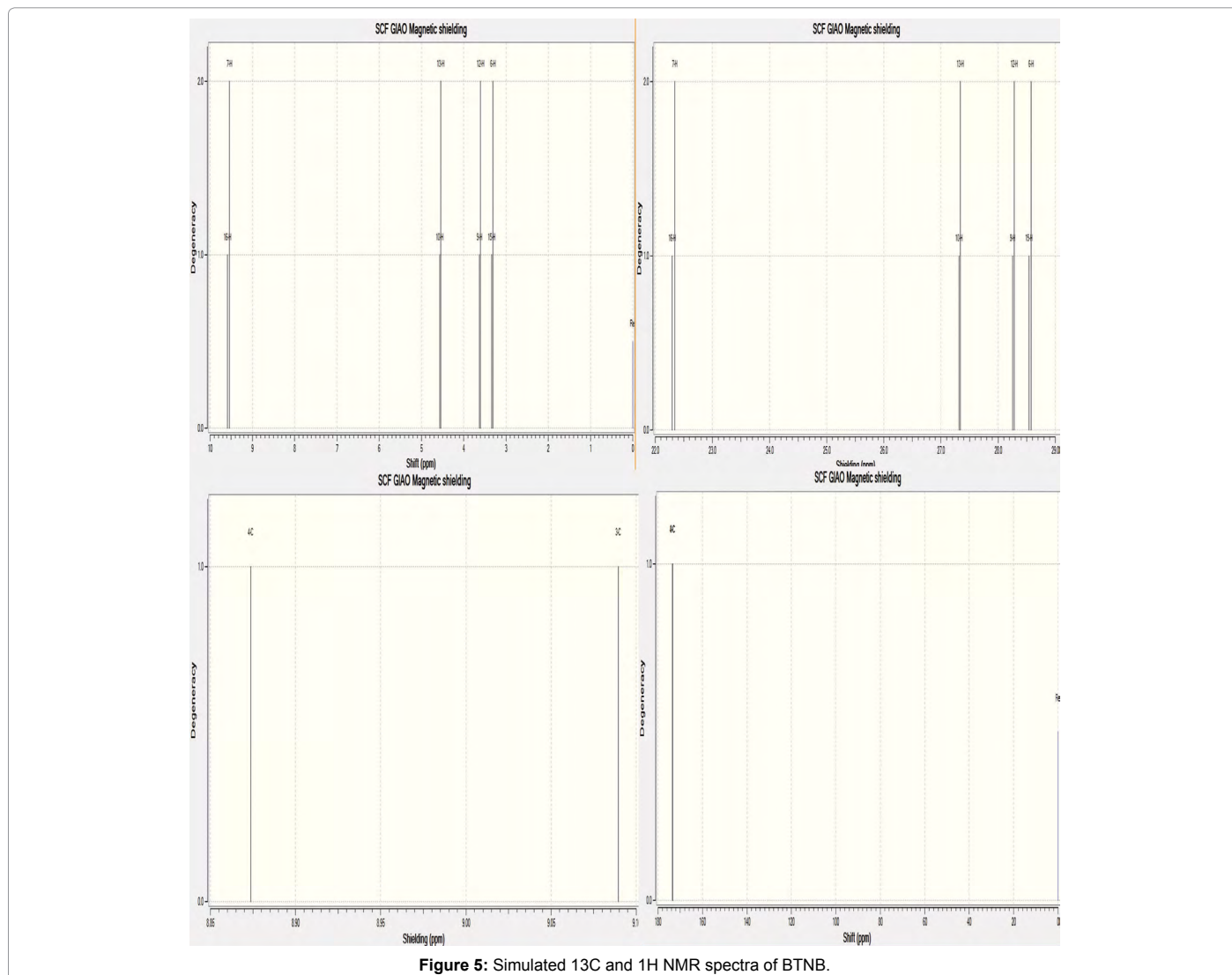


Figure 5: Simulated  $^{13}\text{C}$  and  $^1\text{H}$  NMR spectra of BTNB.



Atom position	B3LYP/6-311+G (d,p) (ppm)	TMS B3LYP/6-311+G (2d,p) GIAO (ppm)	Shift (ppm)	B3LYP/6-311+G (d,p) (ppm)	TMS B3LYP/6-311+G (2d,p) GIAO (ppm)	Shift (ppm)	B3LYP/6-311+G (d,p) (ppm)	TMS B3LYP/6-311+G (2d,p) GIAO (ppm)	Shift (ppm)	B3LYP/6-311+G (d,p) (ppm)	TMS B3LYP/6-311+G (2d,p) GIAO (ppm)	Shift (ppm)
Gas	DMSO			Chloroform			CCl <sub>4</sub>					
S1	650.95	-	650.95	605.85	-	605.85	716.15	-	716.15	689.23	-	689.23
S2	646.13	-	646.13	598.67	-	598.67	710.36	-	710.36	683.80	-	683.80
C3	9.08	173.37	164.29	8.34	174.11	165.77	8.50	173.96	165.46	8.67	173.79	165.12
C4	8.87	173.59	164.72	8.08	174.38	166.30	8.30	174.16	165.86	8.46	174.00	165.54
N5	154.10	-	154.10	145.81	-	145.81	150.90	-	150.90	152.10	-	152.10
N8	156.32	-	156.32	145.73	-	145.73	145.94	-	145.94	150.12	-	150.12
N11	156.364	-	156.364	145.63	-	145.63	145.99	-	145.99	150.16	-	150.16
N14	153.74	-	153.74	145.79	-	145.79	150.74	-	150.74	151.95	-	151.95
H6	28.57	3.30	25.27	27.57	4.31	23.26	28.01	3.86	24.15	28.23	3.64	24.59
H7	22.34	9.53	12.81	22.50	9.38	13.12	22.65	9.22	13.43	22.54	9.34	13.20
H9	28.25	3.62	24.63	27.21	4.66	22.55	27.58	4.30	23.28	27.84	4.03	23.81
H10	27.31	4.56	22.75	26.71	5.17	21.54	26.84	5.03	21.81	27.02	4.85	22.17
H12	28.28	3.60	24.68	27.23	4.65	22.58	27.60	4.28	23.32	27.87	4.01	23.86
H13	27.33	4.54	19.79	26.73	5.14	21.59	26.87	5.00	21.87	27.04	4.83	22.21
H15	28.54	3.34	25.20	27.55	4.33	23.22	27.97	3.90	24.07	28.20	3.68	24.52
H16	22.29	9.58	12.71	22.50	9.38	13.12	22.60	9.27	13.33	22.42	9.39	13.03
Br17	4033.39	-	4033.39	3562.81	-	3562.81	4039.61	-	4039.61	4029	-	4029
Br18	4050.17	-	4050.17	3576.78	-	3576.78	4054.41	-	4054.41	4045	-	4045
Ni19	-16253	-	-16253	-11765	-	-11765	-17430	-	-17430	-16876	-	-16876

Table 5: Calculated <sup>1</sup>H and <sup>13</sup>C NMR chemical shifts (ppm) of Bis(thiourea) Nickel Bromide (BTNB).

## Frontier molecular analysis

The electronic reconfiguration and electronic excitations in frontier molecular orbitals are very much useful for studying the electric and optical properties of the organic molecules. The stabilization of the bonding and destabilization of the antibonding of molecular orbital can be made by the overlapping of molecular orbitals. The stabilization of the bonding molecular orbital and destabilization of the antibonding molecular orbital can increase when the overlap of two orbitals increases [41].

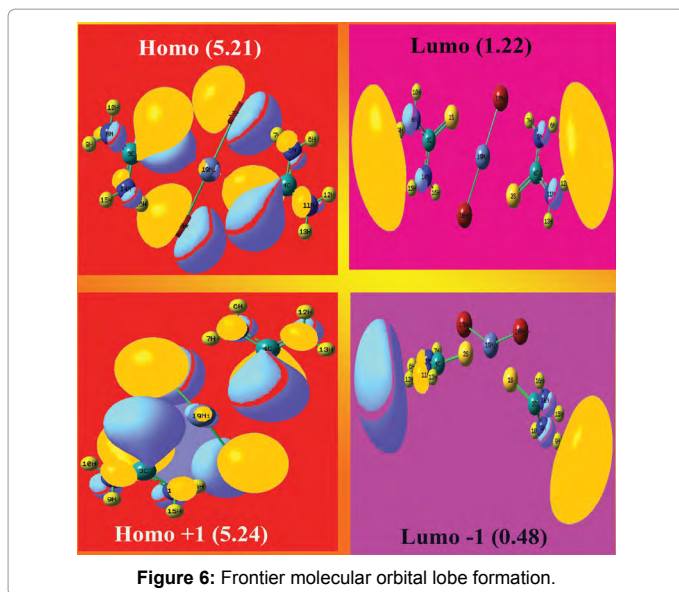
In molecular interaction, there are two important orbitals that interact with each other. One is the highest energy occupied molecular orbital, HOMO which represents the ability to donate an electron. The other is the lowest energy unoccupied molecular orbital which is called LUMO. It has the ability to accept an electron. Hence, HOMO and LUMO are the electron donor and electron acceptor respectively. These orbitals are also called the frontier orbitals. The interaction between them is much stable and is called filled empty interaction. When the two same sign orbitals overlap to form a molecular orbital, the electron density will occupy at the region between two nuclei. The molecular orbital resulting from in-phase interaction is defined as the bonding orbital which has lower energy than the original atomic orbital. The out-of-phase interaction forms the antibonding molecular orbital with higher energy than the initial atomic orbital.

The 3D plots of the frontier orbitals, HOMO and LUMO for the present molecule are in gas and shown in Figure 6. According to such figure, the HOMO is mainly localized over the Nickel, Br, N atoms and

C-S group in which there are two sigma bond interaction taking place over the C-S of thiourea and one delta bond interaction over Nickel bromide. The N and Br atoms of the molecule are connected by S orbital lobes. However, LUMO is characterized by a charge distribution connects the Nickel-bromide atoms and C-S bonds in which there are two sigma and one delta bond interaction taking place. From this observation, it is clear that, the in-phase and out-of-phase interactions are present in HOMO and LUMO respectively. The HOMO→LUMO transition implies an electron density transferred among Nickel bromide and thiourea separately. The HOMO and LUMO energy are 5.21 eV and 1.22 eV in gas phase as shown in Table 6. Energy difference between HOMO and LUMO orbital is called as energy gap (kubo gap) that is important for the stability of structures. The DFT level calculated energy gap is 3.65 eV; it is a medium energy gap and reflects the high electrical activity of the molecule.

## Optical HOMO-LUMO analysis

The UV and visible spectroscopy is used to detect the presence of chromophores in the molecule and shows whether the compound has NLO properties or not. The calculations of the electronic structure of BTNB are optimized in singlet state. The low energy electronic excited states of the molecule are calculated at the B3LYP/6-311++G (d, p) level using the TD-DFT approach on the previously optimized ground-state geometry of the molecule. The calculations are performed in gas phase and with the solvent of DMSO, chloroform and CCl<sub>4</sub>. The calculated excitation energies, oscillator strength (*f*), wavelength (*λ*) and spectral assignments are given in Table 7. The major contributions of the transitions are designated with the aid of SWizard program [42].



Energy levels	Energy in eV
H+8	7.12
H+7	7.03
H+6	6.77
H+5	6.27
H+4	6.21
H+3	5.89
H+2	5.37
H+1	5.24
H	5.21
L	1.22
L-1	0.48
L-2	0.31
L-3	1.31
L-4	1.43
L-5	1.49
L-6	1.97
L-7	2.39
L-8	2.51
L-9	2.75
L-10	2.91

**Table 6:** Frontier molecular orbitals with energy levels of Bis(thiourea) Nickel Bromide (BTNB).

TD-DFT calculations predict that, irrespective of the gas and solvent phase, the entire transitions belong to quartz ultraviolet region. In the case of gas phase, the strong transitions are observed at 981, 408 and 397 nm with an oscillator strength  $f = 0.0002, 0.0008$  and  $0.0435$  with 1.26, 3.03 and 3.12 eV energy gap. The transition is denoted by  $n \rightarrow \sigma^*$  belongs to visible region. The designation of the band is R-band (German, radikalartig) which is attributed to the above said transition of chain of chromophoric groups, such as Nickel bromide group. They are characterized by low molar absorptivities ( $\xi_{\max} < 100$ ) and undergo hypsochromic to bathochromic shift and the solvent effect is inactive in this compound. The simulated UV-Visible spectra in gas and solvent phase are shown in Figure 7.

In the case of DMSO solvent, strong transitions are observed at 1127, 1028 and 381 nm with an oscillator strength  $f = 0.0001, 0.0002$  and  $0.1168$  with maximum energy gap 3.25 eV. They are assigned to  $n \rightarrow \pi^*$  transition and belongs to visible region. One of the electronic

transitions is observed at IR region. This shows that, from gas to solvent, the electronic transitions retained at visible region. This view indicates that, the BTNB molecule has visible active and it is capable of having rich optical properties. In addition to that, the calculated optical band gap is 3.25 eV which also ensure that the present compound possessing LO as well as NLO properties. In view of calculated absorption spectra, the maximum absorption wavelength corresponds to the electronic transition from the HOMO+1 to LUMO-1 with maximum contribution. The Frontier molecular orbital diagram is presented in the Figure 8. In the present compound, the chromophores are Nickel bromide group, so that the crystal properties are enhanced.

The chemical hardness and potential, electronegativity and Electrophilicity index are calculated and their values are shown in Table 8. The chemical hardness is a good indicator of the chemical stability. The chemical hardness of the present compound is 1.82 and therefore, the present compound has much chemical stability. The substitutions of Ni-Br group enhanced the chemical stability and metal character of the compound. Similarly, the electronegativity of the compound is 3.38; the property of chemical bonds in the molecule will be changed from covalent to ionic. Accordingly, due to the addition of Ni, the bonding character of the compound rehabilitated to rich ionic. Electrophilicity index is a factor which is used to measure the energy lowering due to maximal electron flow between donor [HOMO] and acceptor [LUMO]. From the Table 8, it is found that the Electrophilicity index is 3.13 which has high and this value ensures that the strong energy transformation is taking place between HOMO+1 and LUMO-1 instead of HOMO-LUMO since the transition is forbidden between HOMO and LUMO. The dipole moment in a molecule is another important electronic property. Whenever the molecules possess large dipole moment, the intermolecular interactions are very strong. The calculated dipole moment value for the title compound is 4.05 Debye. It is apparent and moderate due to the presence of coordinate covalent bond which is inferred that, the present molecule has strong intermolecular interactions.

### Molecular Electrostatic Potential (MEP) analysis

The molecular electrical potential surfaces illustrate the charge distributions of molecules three dimensionally. This map allows us to visualize variably charged regions of a molecule. Knowledge of the charge distributions is much useful to determine how molecules interact with protein and it can be used to determine the requirement of minimum energy to bind with protein structure [43]. Molecular electrostatic potential view is mapped up at the level of B3LYP/6-311+G(d,p) theory with optimized geometry. There is a great deal of intermediary potential energy, the non red or blue region indicate that the electro negativity difference is not very great. In a molecule with a great electro negativity difference, charge is very polarized in negative and positive form, and there are significant differences in electron density in different regions of the molecule. This great electro negativity difference leads to regions that are almost entirely red and almost entirely blue. The region of intermediary potential is explored by yellow and green colour and the regions of extreme potential look at red and blue colours are key indicators of electronegativity.

The colour code of these maps is in the range between -7.86 a.u. (deepest red) to 7.86 a.u. (deepest blue) in compound. The positive (blue) regions of MEP are related to electrophilic reactivity and the negative (green) regions to nucleophilic reactivity shown in Figure 9. As can be seen from the MEP map of the title molecule, the negative regions are mainly localized on Nickel bromide and sulphur atoms. A maximum positive region is localized on the H of  $\text{NH}_2$  groups indicating

$\lambda$ (nm)	E (eV)	(f)	Major contribution	Assignment	Region	Bands
<b>Gas</b>						
981.66	1.2630	0.0002	H→L (92%)	n→σ*	Visible	R-band (German, radikalartig)
408.02	3.0386	0.0008	H→L-1 (92%)	n→π*	Visible	
397.27	3.1209	0.0435	H+1→L (89%)	n→π*	Visible	
<b>DMSO</b>						
1127.43	1.0997	0.0001	H→L (92%)	n→σ*	Visible	R-band (German, radikalartig)
1028.14	1.2059	0.0002	H→L-1 (92%)	n→π*	Visible	
381.02	3.2540	0.1168	H+1→L (89%)	n→π*	Visible	
<b>Chloroform</b>						
1133.97	1.0934	0.0001	H→L (92%)	n→σ*	Visible	R-band (German, radikalartig)
1015.50	1.2209	0.0002	H→L-1 (92%)	n→π*	Visible	
385.70	3.2145	0.1027	H+1→L (89%)	n→π*	Visible	
<b>CCl<sub>4</sub></b>						
1002.88	1.2363	0.0003	H→L (92%)	n→σ*	Visible	R-band (German, radikalartig)
408.61	3.0343	0.0011	H→L-1 (92%)	n→π*	Visible	
390.62	3.1740	0.0893	H+1→L (89%)	n→π*	Visible	

**Table 7:** Theoretical electronic absorption spectra of Bis (thiourea) Nickel Bromide (BTNB) (absorption wavelength  $\lambda$  (nm), excitation energies E (eV) and oscillator strengths (f) using TD-DFT/B3LYP/6-311++G(d, p) method.

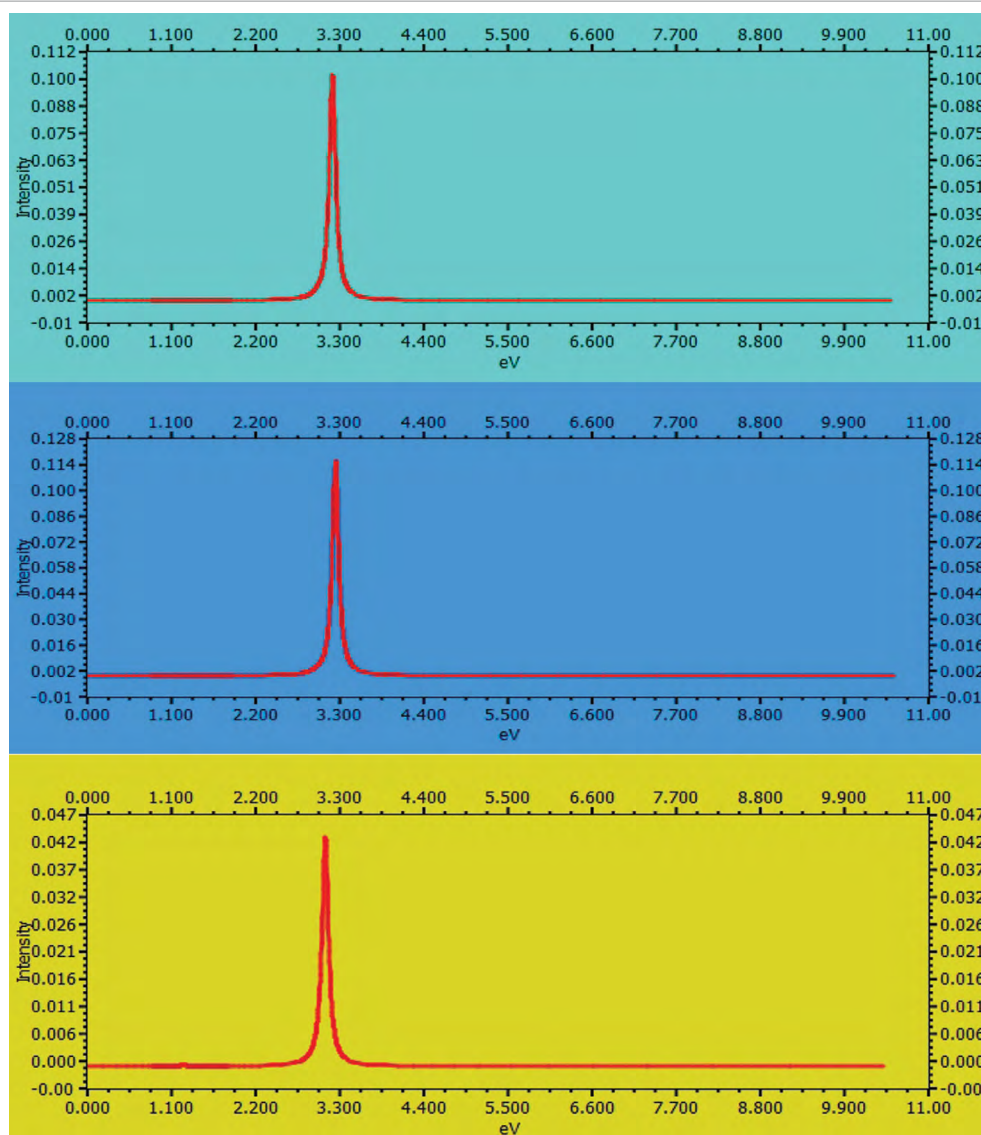


**Figure 7:** Simulated UV-Visible spectra of BTNB.

Parameters	TD-DFT/B3LYP/6-311G++(d, p)
$E_{\text{total}}$ (Hartree)	-7753.11
$E_{\text{HOMO}}$ (eV)	5.2169
$E_{\text{LUMO}}$ (eV)	1.5594
$\Delta E_{\text{HOMO-LUMO gap}}$ (eV)	3.6575
$E_{\text{HOMO-1}}$ (eV)	0.0292
$E_{\text{LUMO+1}}$ (eV)	1.0710
$\Delta E_{\text{HOMO-1-LUMO+1 gap}}$ (eV)	1.0418
Chemical hardness ( $\eta$ )	1.8287
Electronegativity ( $\chi$ )	3.3881
Chemical potential ( $\mu$ )	1.8287
Chemical softness (S)	0.2734
Electrophilicity index ( $\omega$ )	3.1386
Dipole moment	4.0592

**Table 8:** Calculated energies values, chemical hardness, electro negativity, Chemical potential, Electrophilicity index of Bis(thiourea) Nickel Bromide (BTNB).

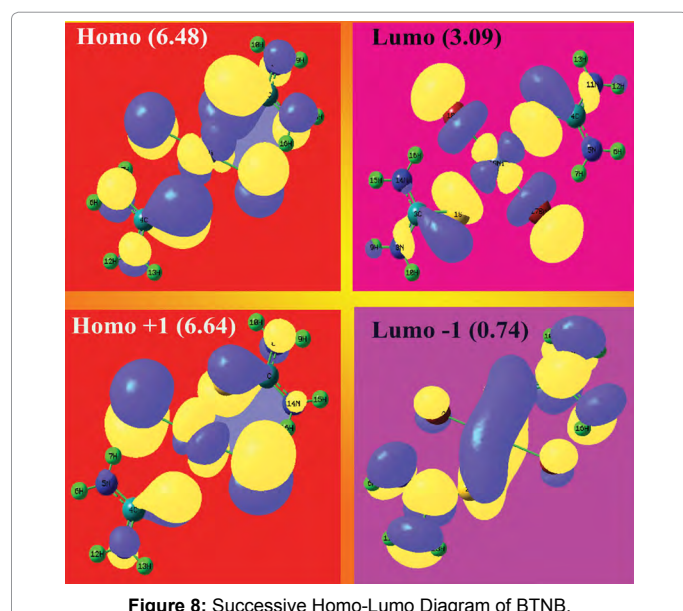


**Figure 8:** Successive Homo-Lumo Diagram of BTNB.

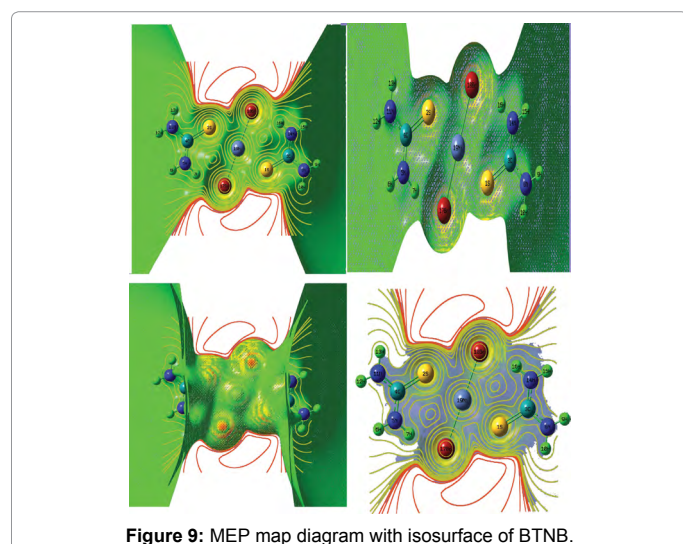


**Figure 9:** MEP map diagram with isosurface of BTNB.

a possible site for nucleophilic attack. Though, this molecule contains different electron rich atoms, the negative potential regions located at metal combined atoms. From these results, it is found that, the metal atoms coupled strongly in the inertial position of organic lattice site.

### Polarizability and first order hyperpolarizability calculations

In order to investigate the relationships among the molecular structures, non-linear optic properties (NLO) and molecular binding properties, the polarizabilities and first order hyperpolarizabilities of the present compound are calculated using DFT-B3LYP method and 6-311+G(d,p) basis set, based on the finite-field approach.

The Polarizability and hyperpolarizability tensors ( $\alpha_{xx}, \alpha_{yy}, \alpha_{zz}, \alpha_{yz}, \alpha_{xz}, \alpha_{zx}$  and  $\beta_{xxx}, \beta_{xyy}, \beta_{yyy}, \beta_{xxz}, \beta_{xyx}, \beta_{yyz}, \beta_{xzz}, \beta_{yzz}, \beta_{zzz}$ ) is obtained from the output file of Polarizability and hyperpolarizability calculations. However,  $\alpha$  and  $\beta$  values of Gaussian output are in atomic units (a.u.) have been converted into electronic units (esu) ( $\alpha$ ; 1 a.u. =  $0.1482 \times 10^{-24}$  esu,  $\beta$ ; 1 a.u. =  $8.6393 \times 10^{-33}$  esu). The mean polarizability ( $\alpha$ ), anisotropy of polarizability ( $\Delta\alpha$ ) and the average value of the first hyperpolarizability  $\langle \beta \rangle$  can be calculated using the equations.

$$\alpha_{\text{tot}} = \frac{1}{3}(\alpha_{xx} + \alpha_{yy} + \alpha_{zz})$$

$$\Delta\alpha = \frac{1}{\sqrt{2}}[(\alpha_{xx} - \alpha_{yy})^2 + (\alpha_{yy} - \alpha_{zz})^2 + (\alpha_{zz} - \alpha_{xx})^2 + 6\alpha_{xz}^2 + 6\alpha_{xy}^2 + 6\alpha_{yz}^2]^{\frac{1}{2}}$$

$$\langle \beta \rangle = [(\beta_{xxx} + \beta_{xyy} + \beta_{zzz})^2 + (\beta_{yyy} + \beta_{yxx} + \beta_{yzz})^2 + (\beta_{zzz} + \beta_{zxx} + \beta_{zyy})^2]^{\frac{1}{2}}$$

It is well known that, molecule with high values of dipole moment, molecular Polarizability, and first hyperpolarizability having more active NLO properties. The first hyperpolarizability ( $\beta$ ) and the component of hyperpolarizability  $\beta_x, \beta_y$  and  $\beta_z$  of BTNB along with related properties ( $\mu_0, \alpha_{\text{total}}$ , and  $\Delta\alpha$ ) are reported in Table 9. The calculated value of dipole moment is found to be 4.05 Debye. The highest value of dipole moment is observed in the component of  $\mu_z$  which is 4.05 D. The lowest value of the dipole moment of the molecule is  $\mu_x$  and  $\mu_y$  component (0.0002 D). The polarization in different coordinate in the material tuned the optical energy that enters. The calculated average Polarizability and anisotropy of the Polarizability is  $275.84 \times 10^{-24}$  esu and  $360.49 \times 10^{-24}$  esu, respectively. In the present molecule, the Polarizability is found to be large in amount. So, the present metallo organic compound is clearly optically active. The high value of Polarizability reflects the rich NLO property of the present compound. The magnitude of the molecular hyperpolarizability  $\beta$ , is one of important key factors in a NLO system. Because, hyperpolarizability of a system induces optical modulation inside the material and it also stimulating second order harmonic generation in the lattice site. The calculated (B3LYP/6-311+G(d,p)) first hyperpolarizability value ( $\beta$ ) is found to be  $60.30 \times 10^{-30}$  esu. The value of hyperpolarizability of the title compound is high and it emphasizes the second order harmonic generation with more amplitude. So, the present compound is able to prepare the NLO crystals for enriched electronic applications.

### Second harmonic generation

The SHG of BTNB crystal was studied using Nd:YAG laser (model continuum YG501C,  $\lambda=1064$  nm) by Kurtz-Perry technique. Powdered sample of the investigated crystal was taken in a glass capillary tube. It was irradiated by the laser pulse and second harmonic signal was detected using an optical cable attached to fluorescence spectroscopy (Princeton instrument Int. Spectroscopy instrument GmbH, model DIDA-512 GIR). The SHG output of the BTNB crystal was found to be 68 mV which is lesser when compared with SHG output of BTCB (98 mV) for laser beam of same intensity. The SHG output confirms the nonlinear nature of the experimental crystal.

Parameter	a.u.	Parameter	a.u.
$\alpha_x$	-25.4048	$\beta_{xxx}$	0.0196
$\alpha_{xy}$	-6.8792	$\beta_{xxy}$	0.0079
$\alpha_{yy}$	-123.9399	$\beta_{yyy}$	0.0002
$\alpha_{xz}$	-0.0056	$\beta_{yyz}$	0.0007
$\alpha_{yz}$	-0.0018	$\beta_{xzz}$	86.4820
$\alpha_{zz}$	-121.1223	$\beta_{xyz}$	1.9418
$\alpha_{tot}$	275.844	$\beta_{yyz}$	6.4666
$\Delta\alpha$	360.496	$\beta_{zzz}$	-0.0091
$\mu_x$	0.0002	$\beta_{yzz}$	-0.0021
$\mu_y$	0.0002	$\beta_{zzz}$	-20.6462
$\mu_z$	4.0592	$\beta_{tot}$	60.3088
$\mu$	4.0592		

**Table 9:** The dipole moments  $\mu$  (D), the polarizability  $\alpha$  (a.u.), the average polarizability  $\alpha$ , (esu), the anisotropy of the polarizability  $\Delta\alpha$  (esu), and the first hyperpolarizability  $\beta$  (esu) of Bis(thiourea) Nickel Bromide (BTNB).

### Thermodynamic properties

Normally, the thermo dynamical analysis on aromatic compound is important since they provide the necessary information regarding the chemical reactivity. In addition to that, it is also very important to discuss the existence and alternation of thermodynamic parameters of the present compound since the molecule favoured with metal-organic substance. On the basis of vibrational analysis at B3LYP/6-311+G(d,p) level, the standard statistical thermodynamic functions: standard heat capacities ( $C_{p,m}^0$ ), standard entropies ( $S_m^0$ ), and standard enthalpy changes ( $\Delta H_m^0$ ) for the title compound were obtained from the theoretical harmonic frequencies and are listed in Table 10 and the correlation graph between heat capacities, entropies, enthalpy changes and temperatures were shown in Figure 10. From the table, it can be observed that, the thermodynamic functions are increased with temperature ranging from 100 to 1000 K due to the fact that the molecular vibrational intensities increases with temperature. From this observation it is clear that, the dissociation of atoms related to the temperature is increased up to 1000 K and the molecule has positive entropy-coefficient. In the case of thermodynamical analysis of the molecule, the enthalpy of a system due to the production of metal ion and organic interactions is found to be increased with consecutive saturation between the successive temperatures (e.g., 300 K – 400 K). At low temperature, it is found that, the specific heat capacity of the present compound falls down rapidly and obeys the Debye  $T^3$  law.

### TGA/DTA analysis

The Thermo Gravimetric Analysis and Differential Thermal Analysis (TGA and DTA) curves for BTNB were obtained by using simultaneous thermo gravimetric analyser (STA) 409C (NETZSCH) at a heating rate of 10°C/minute in nitrogen atmosphere and are reported in Figure 11. The TGA curve shows that there was a weight loss of about 76% in the temperature range 182°C - 607°C. The first endothermic peak at 189.08°C in the DTA curve may be due to the liberation of bromide and the second endothermic peak at 239.18°C may be due to liberation of thiourea in BTNB molecule. The loosely bound nature of bromide in the grown crystal is confirmed by the formation of pale yellow precipitate which is sparingly soluble in ammonia when the powdered sample of the grown crystal is treated with silver nitrate in acid medium. The peaks are observed due to the liberation of bromide and Nickel from the crystal which is due to the weak coordination covalent interaction with thiourea. The formation of the metal complex with thiourea in the inner coordination sphere indicates greater thermal stability of the crystal.

### Microhardness studies

Among the several of hardness measurement, the most common and reliable method is the Vicker's hardness test method. In this method, micro indentation is made on the surface with the help of a diamond pyramidal indenter. Hardness is generally defined as the ratio of the load applied to the surface of the indentation. The Vicker's hardness against load is drawn for BTNB crystals Figure 12. Vicker's microhardness test conducted on the experimental crystal proves its greater physical strength. It is well explained by the increase in hardness value with increase in Load and shown in Table 11.

T(K)	$C_{p,m}^0$ (cal mol <sup>-1</sup> K <sup>-1</sup> )	$S_m^0$ (cal mol <sup>-1</sup> K <sup>-1</sup> )	$\Delta H_m^0$ (kcal mol <sup>-1</sup> )
100.00	399.16	138.97	9.15
200.00	513.97	195.59	26.04
298.15	599.94	235.57	47.30
300.00	601.40	236.21	47.74
400.00	673.70	266.56	72.94
500.00	735.84	290.43	100.84
600.00	790.55	309.59	130.87
700.00	839.49	325.26	162.64
800.00	883.80	338.41	195.84
900.00	924.33	349.71	230.26
1000.00	961.70	359.61	265.73

**Table 10:** Thermodynamic parameters at different temperatures at the B3LYP/6-311++G (d, p) level for Bis(thiourea) Nickel Bromide (BTNB).

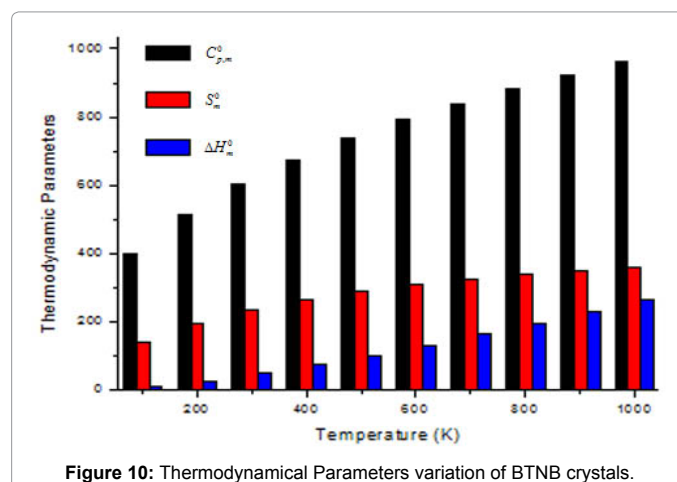


**Figure 10:** Thermodynamical Parameters variation of BTNB crystals.

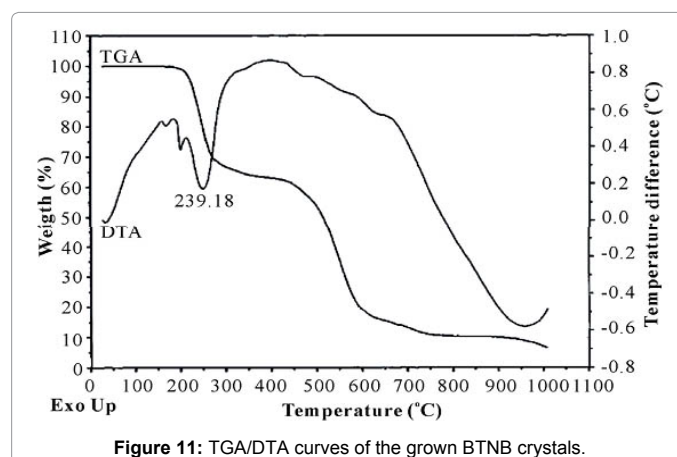


**Figure 11:** TGA/DTA curves of the grown BTNB crystals.

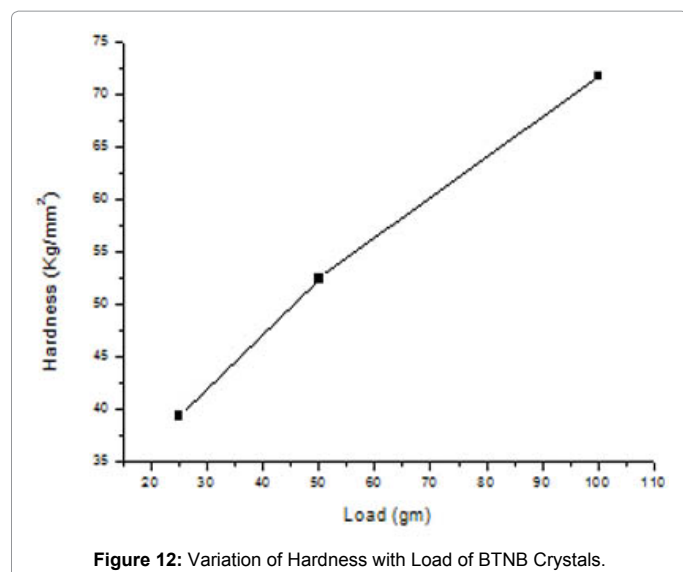


Figure 12: Variation of Hardness with Load of BTNB Crystals.

S No	Load (grams)	BTNB (HV)
1	25	39.3
2	50	52.4
3	100	71.7

Table 11: Microhardness of BTNB crystals.

## Conclusion

The FT-IR, FT-Raman, UV-Vis and NMR spectra have been recorded and the detailed vibrational assignments are presented for BTNB. The complete molecular structural parameters and thermodynamic properties of the compound have been obtained from HF and DFT calculations. The vibrational frequencies of the fundamental modes of the compound have been precisely assigned and analysed and the theoretical results were compared with the experimental vibrations. The single crystals of BTNB, a new semi organic NLO material have been grown from aqueous solution. The chronological change of finger print and group frequency region of the organic part with respect to the functional group (metal bromide) has also been monitored. The change of geometrical parameters along with the substitutions is deeply analyzed. The simulated <sup>13</sup>C NMR and <sup>1</sup>H NMR spectra in gas and solvent phase are displayed and the chemical shifts related to TMS are studied. The electrical, optical and bio molecular properties are profoundly investigated using frontier molecular orbital. From the UV-Visible spectra, it is monitored that, the entire electronic transitions shifted bathochromically due to the substitutional effect. It is also found that the present compound is optically and electrically active and also posses NLO properties. The molecular electrostatic potential (MEP) map is performed and from which the change of the chemical properties of the compound is also discussed. The SHG output confirms the nonlinear nature of the crystal. The TGA/DTA curves and Vicker's microhardness test confirms the thermal stability and physical strength of the investigated crystal.

## References

1. Krishnakumar V, Nagalakshmi R (2007) Crystal growth and characterization of K[CS(NH<sub>2</sub>)<sub>2</sub>]<sub>2</sub>4Br--A semiorganic non-linear optical crystal. *Spectrochim Acta A Mol Biomol Spectrosc* 68: 443-453.
2. Vijayan N, Ramesh BR (2004) Some Studies on the Growth and Characterization of Organic Nonlinear Optical Acetoacetanilide Single Crystals. *Journal of Crystal Growth* 267: 646-653.

3. Kumar RM, Rajanbabu D (2005) Studies on the growth aspects of semi-organic L-alanine acetate: A promising NLO Crystal. *Journal of Crystal Growth* 275: e1935-e1939.
4. Merry HO, Warren LF (1992) Liquid Level Sensor with optical Fibers. *Journal of Applied Optics* 31: 5051.
5. Venkataraman V, Dhavaraj G, Bhat HL (1995) Crystal Growth and Defect Characterization of Zinc Tris(thiourea) Sulfate: A Novel Metal-Organic Nonlinear Optical Crystal. *Journal of Crystal Growth* 154: 92-97.
6. Xu D, Jiao M, Taus Z (1983) A New Phase Matchable NLO Crystal L-Arginine Monohydrate. *Acta Chimica Sinica* 41: 570-573.
7. Ramachandraraja C, Sundararajan RS (2008) Growth, characterization, vibrational spectroscopic and thermal studies of a new metallorganic non-linear optical crystal - Bisthiourea cadmium bromide. *Spectrochimica Acta Part A: Molecular and Biomolecular Spectroscopy* 71: 1286-1289.
8. Venkataraman V, Maheswaran S, Sherwood JN, Bhat HL (1997) Crystal growth and physical characterization of the semiorganic bis(thiourea) cadmium chloride. *Journal of Crystal Growth* 179: 605-610.
9. Hellwege KH, Hellwege AM, Landolt B (1982) Numerical Data and Functional Relationships in Science and Technology Group II. Springer, Berlin.
10. Bhat SG, Dharmaprakah SM (1998) A New Metal-Organic Crystal: Bismuth Thiourea Chloride. *Materials Research Bulletin* 33: 833-840.
11. Karthick N, Sankar R, Jayavel R, Pandi S (2009) Synthesis, growth and characterization of semi-organic nonlinear optical bis thiourea antimony tri bromide (BTAB) single crystals. *Journal of Crystal Growth* 312: 114-119.
12. Lewis RJ (2007) *Sr Hawley's Condensed Chemical Dictionary*. 15th edn. New York, NY: Van Nostrand Reinhold Co.
13. Hartley D, Kidd H (1983) *The Agrochemicals Handbook*. Old Woking, Surrey, United Kingdom: Royal Society of Chemistry/Unwin Brothers Limited.
14. Gerhartz W (1985) *Ullmann's Encyclopedia of Industrial Chemistry*. 5th edn. Deerfield Beach, FL, VCH.
15. Marchewka MK, Pietraszko A (2008) Crystal structure and vibrational spectra of piperazinium bis(4-hydroxybenzenesulphonate) molecular-ionic crystal. *Spectrochimica Acta Part A: Molecular and Biomolecular Spectroscopy* 69: 312-318.
16. Ivan SL, Scuseria GE (2008) The screened hybrid density functional study of metallic thorium carbide. *Chemical Physics Letters* 460: 137-140.
17. Pejov L, Ristova M, Soptrajanov B (2011) Quantum chemical study of p-toluenesulfonic acid, p-toluenesulfonate anion and the water-p-toluenesulfonic acid complex. Comparison with experimental spectroscopic data. *Spectrochimica Acta Part A: Molecular and Biomolecular Spectroscopy* 79: 27-34.
18. Frisch MJ (2009) Gaussian 09, Revision A1, Gaussian, Inc., Wallingford CT.
19. Narayanan B, Bhadbhade MM (2000) Structural studies on Cu(N,N-dialkyldiamine)<sub>2</sub>X<sub>2</sub> complexes: X-ray structure of bis(N-isopropyl-1,2-ethanediamine) copper(II) tetrafluoroborate. *Journal of Molecular Structure (Theochem)* 516: 247-254.
20. Zhengyu Z, Aiping F, Dongmei D (2000) Studies on density functional theory for the electron-transfer reaction mechanism between M-C<sub>6</sub>H<sub>6</sub> and M+-C<sub>6</sub>H<sub>6</sub> complexes in the gas phase. *Journal of Quantum Chemistry* 78: 186-189.
21. Becke AD (1988) Density-functional exchange-energy approximation with correct asymptotic behavior. *Phys Rev A* 38: 3098-3100.
22. Lee C, Yang W, Parr RG (1988) Development of the Colle-Salvetti correlation-energy formula into a functional of the electron density. *Phys Rev B Condens Matter* 37: 785-789.
23. Becke AD (1993) Density-functional thermochemistry. III. The role of exact exchange. *J Chem Phys* 98: 5648-5652.
24. Bellamy LJ (1980) *The Infrared Spectra of Complex Molecules*, Vol. 2, Chapman and Hall, London.
25. Karabacak M, Postalçilar E, Cinar M (2012) Determination of structural and vibrational spectroscopic properties of 2-, 3-, 4-nitrobenzenesulfonamide using FT-IR and FT-Raman experimental techniques and DFT quantum chemical calculations. *Spectrochim Acta A Mol Biomol Spectrosc* 85: 261-270.
26. Silverstein RM, Webster FX (1998) *Spectrometric Identification of Organic Compounds*, 6th edn. Wiley, New York.

27. Pandiarajan S, Umadevi M, Rajaram RK, Ramakrishnan V (2005) Infrared and Raman spectroscopic studies of L-valine L-valinium perchlorate monohydrate. *Spectrochim Acta A Mol Biomol Spectrosc* 62: 630-636.
28. During JR, Bergana MM, Phan HV (1991) Raman and infrared spectra, conformational stability, barriers to internal rotation, ab initio calculations and vibrational assignment of dichloroacetyl fluoride. *Journal of Raman Spectroscopy* 22: 141-154.
29. Varsanyi G (1969) *Vibrational spectra of benzene derivatives*, Academic press, New York.
30. Shanmugam R, Sathayanarayana D (1984) *Spectrochimica Acta A* 40.
31. Silverstein M, Basseler GC, Morill C (1962) Spectrochemtric identification of organic compound. *J Chem Educ* 39: 546.
32. Bellamy LJ, Williams RL (1957) The NH stretching frequencies of primary amines. *Spectrochimica Acta* 9: 341-345.
33. Arjunan V, Mohan S (2009) Fourier transform infrared and FT-Raman spectra, assignment, ab initio, DFT and normal co-ordinate analysis of 2-chloro-4-methylaniline and 2-chloro-6-methylaniline. *Spectrochim Acta A Mol Biomol Spectrosc* 72: 436-444.
34. Swaminathan J, Ramalingam M, Sundaraganesan N (2009) Molecular structure and vibrational spectra of 3-amino-5-hydroxypyrazole by density functional method. *Spectrochim Acta A Mol Biomol Spectrosc* 71: 1776-1782.
35. Nakamoto K (1997) *Infrared and Raman Spectra of Inorganic and Coordination Compounds*, 5th edn. Wiley, New York.
36. Ross SD (1972) *Inorganic Infrared and Raman Spectra*. McGraw- Hill, London.
37. Davidson G (1968) *Vibrational Spectra of Some Coordinated Ligands*. *Spectrosc Prop Inorg Organomet Compds*.
38. *Characteristic Vibrations of Compounds of Main Group Elements I to VIII*, *Spectrosc Prop Inorg Organomet Compounds*.
39. Jean Y, Volatron F (2005) *An Introduction to Molecular Orbitals*. Oxford University Press.
40. Gorelsky SI (2010) *SWizard Program Revision 4.5*, University of Ottawa, Ottawa, Canada.
41. Ramalingam S, Periandy S, Sugunakala S, Prabhu T, Bououdina M (2013) Insilico molecular modeling, docking and spectroscopic [FT-IR/FT-Raman/UV/NMR] analysis of Chlorfenson using computational calculations. *Spectrochimica Acta Part A: Molecular and Biomolecular Spectroscopy* 115: 118-135.
42. Kurtz SK, Perry TT (1968) A Powder Technique for the Evaluation of Nonlinear Optical Materials. *Journal of Applied Physics* 39: 3798-3814.
43. Sundararajan RS, Senthilkumar M, Ramachandraraja C (2013) Growth and Characterization of Bisthiourea Nickel Bromide - New Semiorganic Nonlinear Optical Crystal. *Journal of Crystallization Process and Technology* 3: 56-59.